Contact-less 3D-Coordinate Measurement System by Laser Scanning and Image Reconstruction from Unorganized Data

G. Tognola[(1)], C. Svelto[(2)], M. Parazzini[(1)], P. Ravazzani[(1)], F. Grandori[(1)]
Istituto di Ingegneria Biomedica CNR, c/o Politecnico di Milano,
Piazza Leonardo da Vinci, 32 – 20133 Milan, Italy. Ph: 39 02 2399 3388 – Fax: 39 02 2399 3367
e-mail: Gabriella.tognola@polimi.it
Politecnico di Milano, Dipartimento di Elettronica e Informazione, CNR-IEIIT, and INFM
Via Ponzio, 34/5 – 20133 Milan, Italy. Ph: 39 02 2399 3610 – Fax: 39 02 2399 3413
e-mail: svelto@elet.polimi.it

Abstract-*A simple but robust and efficient 3D laser scanner was developed for data point acquisition from an object surface. The system is mainly developed for digital registration of anatomical parts to be used in biomedical applications. A novel surface reconstruction algorithm is adopted to obtain an explicit 3D model for the measured object with adequate ease and accuracy. Some of the practical applications of this contact-less scanning system, as well as its first step metrological validation are presented.*

Keywords -*3D laser scanner, surface reconstruction, dimensional measurements*

I. INTRODUCTION

The rapid growth of 3D software and hardware for computer visualization and 3D scanning technologies made feasible the acquisition and reconstruction of complex surfaces in many fields, such as reverse engineering, prototyping, 3D printing, manufacturing, medical sciences, terrain mapping, and cultural heritage.

In this paper a custom contact-less 3D-coordinate measurement system, by simple laser scanning of the measurand surface, is described together with a novel image reconstruction algorithm, from unorganized data range. The ensemble of the scanning+reconstruction parts of the system provide for an efficent, reliable, and adequately accurate measurement system aimed at digital resgistration of anatomical surfaces for biomedical applications. After a whole description of the system and its metrological performance, also partly given in previous papers [1-3], we will focus on some specific biomedical applications that take advantage from using such a measurement system. Measurements on objects of well-known geometrical features and dimensions are performed in order to assess accuracy and repeatability levels of this 3D acquisition system. Simulations with a synthetic test surface of a shape similar to a typical ear canal impression determine robustness to noise of the proposed reconstruction algorithm. In the final part of the paper, the first measurements (acquisition + reconstruction) of different surfaces from real objects are presented.

II. THE 3D SCANNING DEVICE

Fig. 1 shows the scanning device developed for this proposed here (see Fig. 1) The hardware apparatus is composed by an high-quality, but still commercial and low-price, He-Ne laser, two CCD cameras and a real-time video processor. During object scanning, a visible laser spot is swept over the object surface

The He-Ne laser (Melles Griot mod. 05LHP121, class IIIa, with 2 mW at 633 nm on a 600 μm spot diameter) provides for a bright but low power, collimated and circular, red spot of excellent spatial profile (Gaussian transverse mode).

The two CCD cameras (MacReflex, mod. 170-157 ver. NP) and the video processor (VP-II, mod. 170-002 ver. 5.0) are both developed by Qualisys (Sweden). Each CCD camera has 604 (H) × 294 (O) picture elements and a frame rate of 60 frames/s. The digital cameras and the video processor used here are very common equipment in biomedical laboratories and were originally developed for motion capture. As a matter of fact, this equipment measures the 3D coordinates of properly illuminated small retro-reflective targets (called markers) attached to a moving subject. Here, the Qualisys system was used to measure the 3D coordinate of an 'active marker', *i.e.*, the laser spot projected over the surface that has to be scanned instead of acquiring the 3D coordinates of passive reflective markers. For a detailed description of the technical functionality of the Qualisys system, see Ref. [4].

Briefly, the 3D coordinate measurement of the light spot is performed in two steps: a) measurement of the 2D position of the light spot on the focal plane of each camera; b) computation of one single 3D coordinate from the two pairs of 2D coordinates, (x_1,y_1) and (x_2,y_2), of the light spot digitized by the two cameras. The video processor makes some processing on the picture taken from each camera in order to find the 2D position of the light spot. Briefly, the video processor is able to find the light spot in a picture that is dark elsewhere. The CCD camera is responsible to make the picture black, except for the light spot. In particular,

this is achieved by the use of an electronic shutter and a variable gain. The shutter causes the image in the camera to become dark, except where there is high intensity light. The variable gain allows to automatically adjust the sensitivity of the camera to match the object with the highest intensity; all other objects will be dark. In this way, the undesired reflections and irrelevant light sources are suppressed. The video processor scans the picture processed by the camera: the camera picture is divided into rows and columns and the transition between dark (i.e., the background) and light are detected together with the light intensity of each pixel. This information on the border position and pixel intensities are used to determine the 2D position of the geometric centroid of the marker. Also, to avoid possible incorrect spot detection, only light spots within a user-defined size are accepted: this allows rejecting both too large light spots (due to sources different from the laser beam) and too small spots (typically due to noise sources). According to the experimental data provided by Qualisys [4], the system resolution in the measurement of the 2D coordinates of passive markers is about 1/30 000 of FOV (field-of-view of the camera across the diagonal), that is about 1/45th of a pixel.

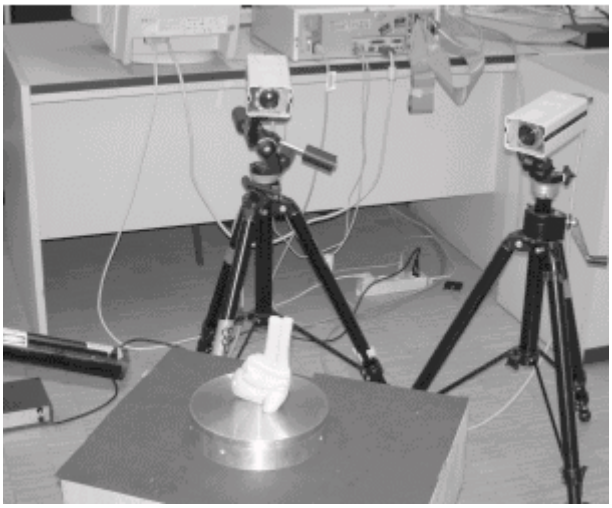

Fig. 1: Experimental set-up during laser scanning. The two CCD cameras are put in front of the object to be scanned; the signal coming out from the cameras is fed to the video processors (not seen in this picture), which in turn are connected to the PC. In this example the object (a human heart model) is put on a turntable. On the leftmost side of the figure, it is possible to see the laser used to scan the object.

Finally, a dedicated data fusion software provides merges the four measured coordinates of the spot, (x_1,y_1) and (x_2, y_2) as seen on the two focal planes of the cameras into a single 3D point (x, y, z) by means of a classical optical triangulation procedure. The registered cloud of unorganized 3D coordinates is the range data to be processed by the proposed reconstruction algorithm. To obtain a complete description of the ear impression surface, object scans from different viewpoints are acquired. This is because the scanning device can acquire only part of the object at a time and/or the object itself may shadow the laser beam reflected from the scanned surface. Classical registration procedures are used to transform the multiple scans of the object into a single coordinate system.

III. The Reconstruction Algorithm

At the end of the scanning and registration procedures, a set of 3D coordinates of the different points, $d_i = \{x_i, y_i, z_i\} \in R^3$ taken from the surface of the measured object is obtained. The original data set $D = \{d_1, \ldots, d_n\}$ consists of completely unstructured points and the object surface is reconstructed by means of a triangular mesh model *M*. The triangular mesh approximating the surface is obtained through an adaptive deformation of a geometrical model [5-6]. Differently from Refs. [5-6], at each iteration, the geometrical model is deformed and re-sampled in a way that it locally minimizes an error function, which gives a quantitative estimate of the accuracy of the reconstruction. The error function is used here to obtain a non-uniform triangular mesh *M* characterized by a greater density of triangles right in those regions of the surface with higher spatial frequency content.

Reconstruction is performed in three phases (for details, see Ref. [1]).

In *phase one* the regular geometric model – an icosahedron – is put inside the volume defined by the range data. The icosahedron is then expanded iteratively until all its vertices reach the boundary of the surface. The effect obtained on the whole geometrical model by this deformation is similar to an inflating balloon. Once the icosahedron has reached its maximum expansion, it is uniformly re-sampled: each triangular face is divided into four faces by connecting the midpoints of its edges. This because the icosahedron has an insufficient number of vertices to properly describe the range data, which usually consists of number of points much higher than those originally available with the icosahedron. In *phase two* the triangular mesh obtained at the end of phase one is locally re-sampled in order to obtain a new mesh richer in details. In *phase three* the mesh is filtered with an iterative low-pass, non-shrinking filter [7]. While filtering, the vertices are moved without changing the connectivity, the number of vertices and triangles of the mesh. At the end of the filtering process, a new smoothed mesh M_3 is obtained, which is the 3D model of the measured object.

IV. VALIDATION OF THE MEASUREMENT SYSTEM

All the measurements described in this paper were done using a calibration volume of 30×30×30 cm^3 and standard Cosmicar 8.5 mm lenses for the cameras, with an horizontal FOV of 39°.

In a first set of experiments, a steady laser spot was shined on a reference plane and the three coordinates of such a steady and elementary point were repeatedly registered at 60 Hz acquisition rate, for a total of 32 000 repeated measurements of the laser spot. The standard deviations of the registered 3D coordinates of the static point in the x, y, z directions were 13.9 μm, 11.5 μm, and 10.6 μm, respectively, with a system resolution $\Delta x=\Delta y=\Delta z=9.33$ μm and giving a measurement repeatability of ~50 μm. As a further experiment to assess the performance of the scanning device, a reference solid sphere of dimensions (~2 cm diameter) similar to a real ear impression was used. In this case a portion of the solid surface was scanned and acquired. From the registered 3D range data the best-fit theoretical sphere was calculated with a least square procedure minimizing the average distance between the fitting sphere and the experimental points. A solid sphere of radius 11.133±0.016 mm, as measured from 20 repeated measurements by a 50 μm resolution caliper, was used as the reference sphere to be scanned and acquired. Ten repeated acquisitions of the object were performed (each acquisition consisted of about 3 500 points obtained from laser scanning the sphere) and the radius of the best-fit sphere was calculated for each acquisition: the average value of the radius was 11.147 mm with 0.016 mm statistical uncertainty, resulting in good compatibility (k=1 coverage factor) with the corresponding mechanical measurement. The acquisition noise for this 11-mm-radius sphere was almost identical in all the 10 repeated measurements and equal to ~171 μm.

To give an application-oriented measure of the accuracy of the reconstruction algorithm alone, a synthesized test surface was used, with shape and dimensions similar to a real ear impression. To test the performance and the robustness to noise of the reconstruction algorithm, a Gaussian noise of increasing rms amplitudes was added to the original test surface. As an example, Fig. 2 shows the original synthesized surface, the noisy surface, and the reconstructed surface. The range data obtained from the noisy surface was fed to the reconstruction algorithm and the point-to-point reconstruction error between the original test surface and the reconstructed surface was evaluated. In all test conditions, *i.e.* for added rms noise values from 170 μm up to 1 mm, the reconstruction error was significantly below the level of noise added to the original synthetic surface. In particular, for a level of noise equal to the acquisition noise, *i.e.* 170 μm, the rms reconstruction error was equal to 100 μm, resulting in the smallest noise reduction factor (~1.7) whereas at higher noise levels a greater noise reduction is achieved (*e.g.* for 1 mm rms added noise the result is ~480 μm rms noise with a reduction factor of ~2.1).

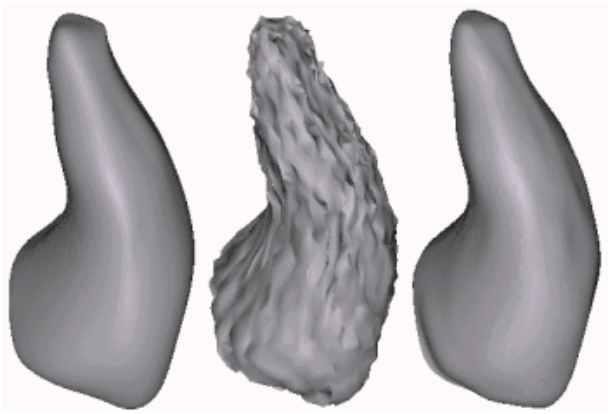

Fig. 2: Pictorial example of the reconstruction accuracy of the proposed algorithm. *Left*: Original test surface whose shape and dimensions resemble a real ear impression. *Middle*: The noisy surface obtained from the original test surface by adding a Gaussian noise of 170 μm (rms value). *Right*: The reconstructed surface obtained by processing the range data derived from the noisy surface.

V. RECONSTRUCTION OF ANATOMICAL SURFACES

Results obtained from the acquisition and reconstruction of a model of a heart, 1:1 scale, and a real ear canal impression, used in the industrial process of hearing aids manufacturing, are presented in Figs. 3 and 4, respectively. Very recently, the molder of a human dental arch was acquired by the described 3D laser scanner obtaining a range data 'dental arch' consisting of 89 029 points. Fig. 5 shows the input range data taken from the scans of the dental arch of the same patient before and after a teeth alignment orthodontic treatment (panels a and c), and the resulting final reconstructed surfaces (panels b and d). The two surfaces here obtained (92 443 triangles for panel b and 59 853 triangles for panel d) were used in clinical routine to quantify the point-to-point difference between the dental arch shape before and after the orthodontic treatment and to determine the position of the dental arch areas where the greatest differences were located.

In all cases the reconstructed surfaces have enough resolution and geometrical accuracy to allow quantitative measurements useful for biomedical (diagnostic and pre-operative surgical planning) and industrial (design of optimally fitted prosthetic devices) applications.

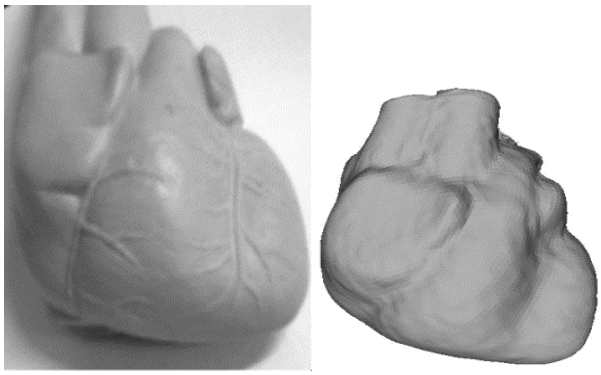

Fig. 3: *Left*: Original model of a human heart (70×104×99 mm^3). *Right*: Solid representation of the reconstructed 3D surface of the heart model.

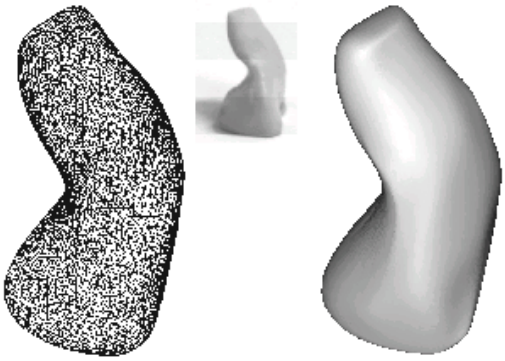

Fig. 4: *Left*: Range data (point cloud) obtained from the acquisition of the object surface. *Middle*: Real ear impression (18×14×22 mm^3) *Right*: Solid representation of the reconstructed

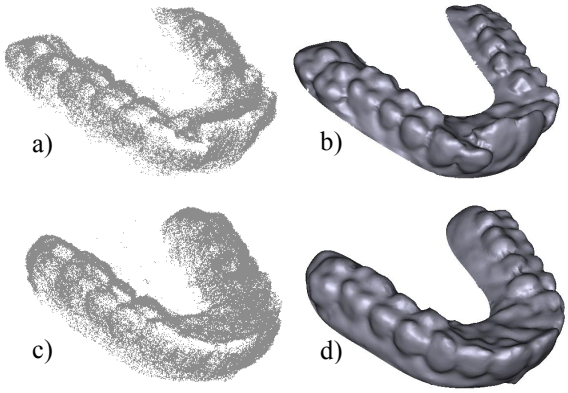

Fig. 5: a, c) Clouds of acquired points (unorganized range data) from the dental arch (50×60×10 mm^3) of a patient before and after the alignment treatment. b, d) Solid representation of the final reconstructed 3D models.

VI. Conclusions

A contact-less 3D-coordinate measurement system was developed together with a novel surface reconstruction algorithm aimed at digital registration of anatomical surfaces to be used in biomedical applications. The system performance was validated by acquiring and reconstructing different reference surfaces, both real and synthetic. The most promising biomedical application of the system developed are for the design of custom-made prosthetic devices (such as for hearing aids, orthopedic prostheses, and orthodontic devices), for monitoring the morphological time evolution of accessible anatomical parts in comparison to the corresponding non-pathological behavior (such as during the recovery after a surgical treatment), and in general for surgical planning.

References

[1] G. Tognola, M. Parazzini, C. Svelto, P. Ravazzani, F. Grandori, "A fast and reliable system for 3D surface acquisition and reconstruction", Image and Vision Computing, 2003 (in press).

[2] G. Tognola, M. Parazzini, P. Ravazzani, F. Grandori, C. Svelto, "Simple 3D laser scanner for anatomical parts and image reconstruction from unorganized range data", proc. IEEE IMTC Conf., Anchorage, 2002, pp. 171-174.

[3] G. Tognola, M. Parazzini, P. Ravazzani, C. Svelto, and F. Grandori, "3D reconstruction of anatomical surfaces from unorganized range data", proc. of the 23rd Annual International Conference of the IEEE EMBS, Istanbul (Turkey), vol. 3, pp. 2534-2536, 2001.

[4] T. Josefsson, E. Nordh, P-O. Eriksson, "A flexible high-precision video system for digital recording of motor acts through lightweight reflex markers", Computer Methods and Programs in Biomedicine, vol. 49, pp. 119-129, 1996.

[5] A.J. Bulpitt, N.D. Efford, "An efficient deformable model with a self-optimising mesh", Image and Vision Computing, vol. 14, pp. 573-580, 1996.

[6] J.V. Miller, D.E. Breen, W.E. Lorensen, R.M. O'Bara, M.J. Wozny, "Geometrically deformed models", Computer Graphics, vol. 25, pp. 217-226, 1991.

[7] G. Taubin, "A signal processing approach to fair surface design", Computer Graphics, pp. 351-358, 1995.

[8] L.G. Brown, "A survey of image registration techniques", ACM Comp. Survey, vol. 24, pp. 325-376, 1992.

[9] M. Algorri and F. Schmitt, "Surface Reconstruction from Unstructured 3D Data", proc. of Computer Graphics Forum, vol. 15, pp. 47-60, 1996.

[10] H. Hoppe, T. Derose, T. Duchamp, J. McDonalds, and W. Stuelzle, "Surface reconstruction from unorganised points", proc. of Computer Graphics (SIGGRAPH), pp. 19-26, 1993.